Advanced Engineering Letters **Vol.4, No.1, 21-30 (2025)** **e-ISSN: 2812-9709**

FEASIBILITY STUDY ON POWERING CATHODIC PROTECTION SYSTEMS WITH SOLAR ENERGY

UDC:621.383.5:620.197.5
Original scientific paper https://doi.org/10.46793/adeletters.2025.4.1.3

Șerban Bunda[1], Simona Dzitac[1*]

[1]University of Oradea, Faculty of Energy Engineering and Industrial Management, Oradea, Romania

Abstract:
The aim of the paper is to evaluate the feasibility of powering impressed current cathodic protection systems using solar energy. For this purpose, a solar system with battery storage was designed to power the cathodic protection system, calculating both the initial investment costs and the costs over the entire lifespan of the system. Additionally, the costs required to extend the low-voltage grid to power the designed system were determined, and a comparison was made between the two power supply methods in terms of costs and distances to the connection point with the electrical system. Finally, the main conclusions regarding the feasibility of the two methods and their importance in practical applications were highlighted. The most cost-efficient system over the considered lifetime is the one that uses Li-based batteries and a minimum number of electric support poles. The results show that the use of ICCP systems powered by photovoltaic panels with battery storage (PV-BA) is feasible when the distance to the connection point with the grid exceeds 4 km.

ARTICLE HISTORY
Received: 19 January 2025
Revised: 3 March 2025
Accepted: 24 March 2025
Published: 31 March 2025

KEYWORDS
Solar energy, Energy storage, Corrosion, Cathodic protection, Cathodic Protection system, Photovoltaic system, Cost calculation

1. INTRODUCTION

Solar energy, captured through photovoltaic (PV) panels, plays a crucial role in providing sustainable and renewable energy solutions [1,2]. By converting sunlight into electricity, PV panels offer an environmentally friendly and cost-effective alternative to traditional energy sources, reducing dependence on fossil fuels and contributing to environmental protection [3,4].

In cathodic protection systems, solar energy ensures a reliable and independent power supply, especially in remote areas with no or limited access to the national grid [5]. The use of solar energy in cathodic protection systems is a cost-effective alternative, providing clean and reliable electricity generation over long periods, making it a vital component in modern energy solutions [6].

Corrosion is a natural process that causes metallic materials to degrade due to electrochemical reactions with the surrounding environment [7-9]. This phenomenon can have negative consequences on the integrity and durability of metallic structures, especially those buried underground, such as gas/oil pipelines, water networks, and underground reservoirs. Corrosion not only reduces the lifespan of these structures but can also lead to significant economic losses and environmental risks.

Various protection methods are used, including Impressed Current Cathodic Protection (ICCP) to prevent and control the harmful effects of corrosion. This electrochemical technique involves applying an electric current from an external power source through the environment and onto the metallic structure it protects [9]. This current modifies the environment around the buried metal structure, thereby stopping the corrosion process.

ICCP is used for cathodic protection due to this method's advantages: longer anode lifespan, greater control over the current supplied to the anodic system, easier monitoring and control of CP, and, in the long term, it can be much more cost-effective [10].

*CONTACT: Simona Dzitac, e-mail: simona.dzitac@gmail.com

However, to ensure the effectiveness of the method, the ICCP system requires regular monitoring and maintenance, as well as periodic adjustments, depending on environmental changes [9].

Usually, the power supply for ICCP systems is provided by connecting it to the low-voltage electrical grid of the national power system in accordance with the current standards. Fig. 1. shows the usual method of powering from the national grid as well as the ICCP system's main components.

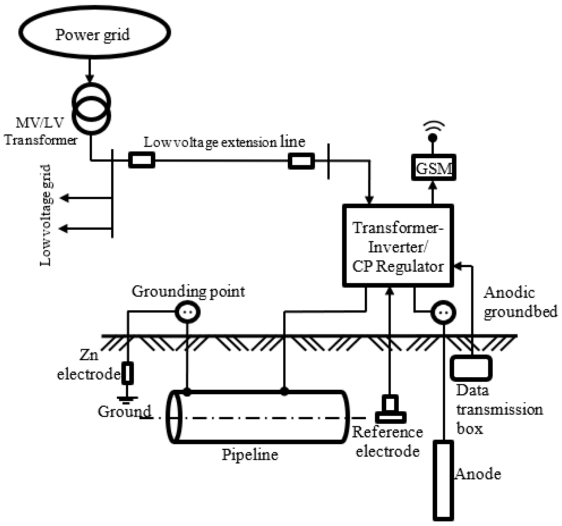

Fig. 1. The main components of an ICCP system

Using solar resources to power ICCP systems is ideal for buried metallic structures located in completely isolated areas, far from the electrical grid. The main components of such a system are shown in Fig. 2.

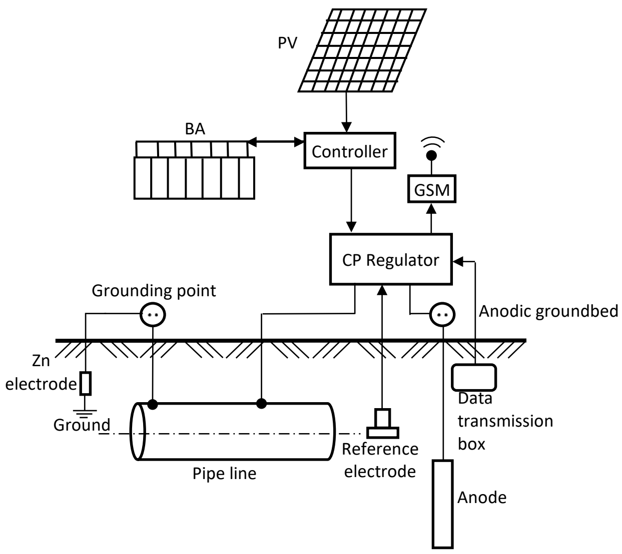

Fig. 2. The PV system components powering ICCP system

2. THE CASE STUDY

As a case study, a pipeline for transporting hydrocarbons from the pumping station to the collection tanks located in the Marghita area in the northwest part of Bihor County is considered. The parameters of the pipeline are summarized in Table 1.

Table 1. Steel pipeline characteristics for the considered case study

Standard pipeline type DN150	
Pipeline length (*L*)	5 km
Exterior diameter (*D*)	168.3 mm^2
Maximum flow (*q*)	100 m^3/h
Maximum speed (*v*)	1.2 m/s
The current density required for permanent CP (*J*)	0.4 mA/m^2
Insulation	Extruded polyethylene

For the pipeline located at coordinates α = 47.33° N latitude and *L* = 22.29° E longitude, according to [11], the average monthly insolation (*H*) at the specific tilt angles of the PV system is given in Table 2.

Table 2. *H* (kWh/m²/day) at the specific tilt angles [11]

Month	$\alpha = \phi$ -15°	$\alpha = \phi$	$\alpha = \phi$ +15°
January	2.1	2.3	2.6
February	3.1	3.3	3.6
March	4.6	4.7	5.1
April	2.6	5.7	6.1
May	6.6	6.7	7.1
June	7.1	7.2	7.6
July	7.0	7.0	7.1
August	6.5	6.6	6.6
September	5.1	5.3	5.1
October	4.0	4.1	4.1
November	2.6	2.7	3.1
December	2.1	2.3	2.6

From Fig. 2, it can be observed that the power source for the ICCP system must provide the following required currents:

- The required cathodic protection current, I_{CP};
- The current for the protection of zinc anodes used for grounding connections of the pipeline, I_{aZn};
- The current for the CP regulator, which ensures control, command, and data telemetry, I_{CPreg};
- The current for data telemetry of the potential probe, I_{DT}.

Thus, the calculation equation for the total current required by the system will be:

$$I_{tot} = I_{CP} + I_{aZn} + I_{CPreg} + I_{DT} \quad (1)$$

3. DESIGN OF THE POWER SUPPLY SYSTEM BASED ON PV RESOURCE

3.1. Calculating the Total Required Current

The sizing of this current is based on the protective current density, which for new pipelines insulated with extruded polyethylene, is J = 0.4 mA/m² = 0.0004 A/m². This value also includes the aging factor. Thus, with data from Table 1 for the 5 km standard DN150 pipeline, the required CP current is [12]:

$$I_{CP} = J \cdot \pi \cdot D \cdot L = 0.0004 \cdot 3.1416 \cdot 0.1638 \cdot 5000 = 1.057\ A \quad (2)$$

For grounding the pipeline, zinc anodes will be used, having the characteristics listed in Table 3.

Table 3. Zinc grounding electrode characteristic for pipeline protection [5]

Standard Zinc anode for pipeline grounding	
Anode length (L_{Zn})	1 m
Anode width (l_{Zn})	0.03 m
The exterior area (S_{Zn})	0.122 m^2
Current density for the surfaces of uncoated anodes (J_{Zn})	0.01 A/m^2

Since the grounding of the pipeline is performed at its ends, at the current injection point of the anodes, and at a maximum of 10 km along the pipeline [12], this results in 3 grounding points, and consequently, the need for n_{Zn} = 3 zinc anodes.

Therefore, the total surface area of the zinc anode will be calculated as:

$$S_{totZn} = S_{Zn} \cdot n_{Zn} = 0.122 \cdot 3 \cong 0.366\ \text{m}^2 \quad (3)$$

Thus, the current for the protection of zinc anodes used for grounding connections of the pipeline will be:

$$I_{aZn} = J_{Zn} \cdot S_{totZn} = 0.01 \cdot 0.366 \cong 0.04\ A \quad (4)$$

Considering the data telemetry equipment as well as the GSM/internet communication equipment along with the control and command unit, the required current is estimated not to exceed I_{CPreg} = 0.45 A. (5)

Since each potential probe will be equipped with a data telemetry box and the number of potential probes will be n_{pp} = 4 (one at the I_{CP} insertion point and 3 at each grounding point), the current required for the telemetry of the potential probes will be [12]:

$$I_{DT} = n_{pp} \cdot I_{pp} = 4 \cdot 0.02 = 0.08\ A \quad (6)$$

In which I_{pp} = 0.02 A represents the required current for a single potential probe.

Considering the relations 1, 4, 5, and 6, the total current required by the CP system will be:

$$I_{tot} = 1.057 + 0.004 + 0.45 + 0.08 = 1.6\ A \quad (7)$$

3.2. Sizing of the Anodic Groundbed

Due to their durability and efficiency in generating the current required for cathodic protection, Mixed Metal Oxide (MMO) tubular anodes are chosen. Their technical characteristics are presented in Table 4.

Table 4. Tubular MMO anode characteristics [12]

MMO anode for pipeline CP	
Anode length (L_{MMO})	1.2 m
Anode diameter (φ_{MMO})	0.032 m
Current density (δ_{MMO})	100 A/m^2
Lifespan (D_{MMO})	25 years

From Table 4, the surface area of the MMO anode will be calculated as:

$$S_{MMO} = \pi \cdot \varphi_{MMO} \cdot L_{MMO} = 3.1416 \cdot 0.032 \cdot 1.2 = 0.12\ m^2 \quad (8)$$

It follows that the current supplied by an MMO anode will be:

$$I_{MMO} = \delta_{MMO} \cdot \varphi S_{MMO} = 100 \cdot 0.12 = 12\ A \quad (9)$$

Considering that for MMO anodes the consumption rate of the anodic material is very low, m = 0.0001 kg/A year, and that the utilization factor is u = 0.85 (dimensionless), the current at the end of the anodes' life is calculated to be:

$$I_{end} = I_{CP} \cdot (1 + S_f) = 1.057 \cdot (1 + 0.85) = 1.32\ A \quad (10)$$

Where S_f is the safety factor considered as 0.25 for normal soil without difficult conditions [12,13]. For simplification of the calculations, the pipeline is considered to be buried in normal soil, without difficult conditions. In case different types of soil are encountered, the corresponding coefficients are applied.

The sizing of the anodic mass is done using Eq.(11):

$$M_{MMO} = m \cdot I_{end} \cdot \frac{D_{MMO}}{u} = 0.0001 \cdot 1.32 \cdot \frac{25}{0.85} = 0.0038\ kg \quad (11)$$

The capacity of a single MMO anode will be:

$$C_{MMO} = I_{MMO} \cdot D_{MMO} = 12 \cdot 25 = 300\ A \quad (12)$$

Thus, the number of MMO anode required must be greater than N:

$$N_{MMO} = \frac{I_{end}}{D_{MMO} \cdot C_{MMO}} = \frac{1.32}{25 \cdot 300} = 0.11 \qquad (13)$$

Eq.(13) results that a single MMO anode is necessary for CP. However, in practice, two anodes are always used. For a uniform distribution of the protection current and to maintain the pipeline potential within safe limits, the two anodes (thus the two anodic groundbeds can be positioned at the ends of the pipeline, in this case, each anodic groundbed covering 2.5 km of the pipeline [12,13].

Additional injection points may be required to ensure adequate protection if there are non-uniformities in the soil. However, in this configuration with two electrodes, two injection points are sufficient.

Considering the calculations performed so far, it follows that the total CP current required for 25 years of operation will be:

$$I_{tot} = I_{CP} + I_{aZn} + I_{CPreg} + I_{DT} = 1.32 + 0.004 + 0.45 + 0.8 = 1.9 \text{ A} \qquad (14)$$

To ensure the reliability, efficiency, and durability of the system, as well as to avoid issues caused by undersizing or unexpected conditions, the obtained values are rounded up, so I_{tot} = 2 A.

3.3. Calculating the Daily Load

Since the photovoltaic system and energy storage system must support the total protection current throughout the entire day, the amp-hour load per day is calculated as [13]:

$$I_{day} = I_{tot} \cdot 24 = 2 \cdot 24 = 48\ A \qquad (15)$$

Taking into account the cable losses and the energy storage subsystem losses, for which the implicit design values of ΔP_{cable} = 0.98 respectively ΔP_{BA} = 0.9 have been considered, the corrected value of the daily load will be:

$$I_{cor} = I_{day} \cdot \Delta P_{cable} \cdot \Delta P_{BA} = 2 \cdot 0.98 \cdot 0.9 \cong 55\ Ah/day \qquad (16)$$

3.4. Calculating of the Optimal Tilt Angle for Photovoltaic Panels

Considering that the solar irradiance of the location is obtained and presented in Table 2, the peak sun hours per day (N) can be calculated using Eq.(17):

$$N = \frac{H}{1000} \quad \left(\frac{h}{day}\right) \qquad (17)$$

It follows that the design current is calculated as:

$$I_{des} = I_{cor} \cdot N \qquad (18)$$

Considering the data from Table 2 and Eq.(18), the design current for each month of the year and the three specific tilt angles of the PV modules are obtained, as shown in Table 5.

Table 5. Design current for specific PV tilt angle

Month	H (h/day)	I_{des} (A)	H (h/day)	I_{des} (A)	H (h/day)	I_{des} (A)	H (h/day)	I_{des} (A)
	α = ϕ -15⁰		α = ϕ		α = ϕ		α = ϕ +15⁰	
Jan	2.1	26.2	2.3	23.9	2.3	23.9	2.6	21.2
Feb	3.1	17.7	3.3	16.7	3.3	16.7	3.6	15.3
Mar	4.6	12.0	4.7	11.7	4.7	11.7	5.1	10.8
Apr	2.6	21.2	5.7	9.6	5.7	9.6	6.1	9.0
May	6.6	8.3	6.7	8.2	6.7	8.2	7.1	7.7
June	7.1	7.7	7.2	7.6	7.2	7.6	7.6	7.2
July	7.0	7.9	7.0	7.9	7.0	7.9	7.1	7.7
Aug	6.5	8.5	6.6	8.3	6.6	8.3	6.6	8.3
Sept	5.1	10.8	5.3	10.4	5.3	10.4	5.1	10.8
Oct	4.0	13.8	4.1	13.4	4.1	13.4	4.1	13.4
Nov	2.6	21.2	2.7	20.4	2.7	20.4	3.1	17.7
Dec	2.1	26.2	2.3	23.9	2.3	23.9	2.6	21.2

From Table 5, the highest design current for each tilt angle and the corresponding solar maximum are selected [13], considering only the critical months, in our study case being the winter months of December and January. The results are summarized in Table 6.

Table 6. Tilt angle and corresponding I_{pr} for critical months

α = 37.33°		α = 47.33°		α = 57.33°	
N **(h/zi)**	I_{pr} **(A)**	***N*** **(h/zi)**	I_{pr} **(A)**	***N*** **(h/zi)**	I_{pr} **(A)**
2.1	26.2	2.3	23.9	2.6	21.2

The optimal tilt angle of the PV modules is obtained by selecting the smallest value of I_{des} from Table 6, that is α = 57.330 at N = 2.6 h/day for I_{des}= 21.2 A.

3.5. Determining the Nominal Voltage of the PV System

For this purpose, the resistance of the MMO anode was first calculated as:

$$R = \frac{\rho}{2\pi \cdot L} \cdot ln\frac{4L}{\Phi} = \frac{20}{2\pi \cdot 1.2} \cdot ln\frac{4 \cdot 1.2}{\Phi 0{,}032} = 13.3\Omega \qquad (19)$$

Where the component of the equation is taken from subsection 3.2:

ρ - soil resistivity = 20 Ω·m,

L - anode length = 1.2 m,

Φ - anode diameter =0.032 m^2.

The nominal voltage will be:

$$U = I_{CP} \cdot R = 1.057 \cdot 13.3 \cong 14V \qquad (20)$$

Due to the fact that there is no standard voltage of 14 V, the nominal voltage for the CP power supply system is chosen to be U_{nCP} = 24 V DC.

3.6. Sizing the Battery Bank System

For sizing the battery bank, the starting point is I_{cor} = 55 A, calculated in Section 3.3, and a storage period of 14 days is considered to ensure a system availability of 99% for 2.6 peak sun hours per day, as shown in Fig. 3.

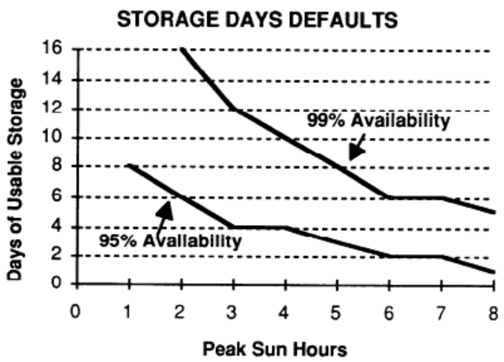

Fig. 3. Recommended storage days at different peak sun hours per day [13]

To avoid overloading the battery and increase its lifespan, the maximum allowable discharge is considered to be D_{Max} = 0.75 [14,15]. Additionally, the derate factor for temperature is considered K_{tBA} = 15 for winter conditions, Table 7.

With these data, the battery capacity required to meet the daily load for the required number of days is obtained as C_{reqBA} = 685 Ah.

Table 7. Derate for temperature for the BA

Temperature		K_{TBA}
ºC	ºF	
6.7	80+	1.00
21.2	70	1.04
15.6	60	1.11
10	50	1.19
4.4	40	1.30
1.1	30	1.40
-6.7	20	1.59

At this stage of sizing, two types of BA can be chosen: lead-acid based, which is cheaper, and lithium based, which is more expensive but have a longer lifespan.

For lead-acid batteries of the Trojan T105 type, with the technical data presented in Table 8, the following results are obtained:

- Number of batteries in parallel N_{parBA} = 4,
- Number of batteries in series N_{serBA} = 2,
- Total number of batteries N_{totBA} = 8,
- System BA capacity C_{sysBA} = 1000 Ah,
- Usable system BA capacity C_{useBA} = 750 A.

The value that covers the requested capacity of 685 Ah.

Table 8. The chosen lead-acid battery type characteristics [16]

Trojan T105			
Characteristics	**Symbol**	**Value**	**Unit**
Nominal voltage	U_{nBA}	2x6=12	(V)
Rated capacity	C_{selBA}	250	(Ah)
Price	P_{BA}	317	($)

For lithium-based batteries of the LiFePO4 type, with the technical data presented in Table 9, the following results are obtained:

- Number of batteries in parallel N_{parBA} = 5,
- Number of batteries in series N_{serBA} = 1,
- Total number of batteries N_{totBA} = 5,
- System BA capacity C_{sysBA} = 1000 Ah,
- Usable system BA capacity C_{useBA} = 750 Ah.

The value that covers the requested capacity of 685 Ah.

Table 9. The chosen lead-acid battery type characteristics

Advanced Energy System (AES) LiFePO4			
Characteristics	**Symbol**	**Value**	**Unit**
Nominal voltage	U_{nBA}	24	(V)
Rated capacity	C_{selBA}	200	(Ah)
Price	P_{BA}	926	($)

3.7. PV System Sizing

The starting point for sizing the PV system is the design current I_{des} = 21.2 A, calculated in subsection 3.4. Taking into account the module derate factor with a temperature of 0.9 (default value for polycrystalline PV panels), the derated design's current result is I_{ddes} = 23.6 A.

From the manufacturers' catalogues, ECO-MEM 50316 solar panels are chosen for the PV system, and their technical specifications are presented in Table 10.

Table 10. The chosen PV panel characteristics [17]

Bauer Polycrystalline BS215-6P2			
Characteristics	**Symbol**	**Value**	**Unit**
Rated Power	P_{PV}	300	(W)
Rated module current	I_{nPV}	7.85	(A)
Module derated factor	DF	0.9	-
Voltage required for load	U_{load}	24	(V)
Highest temp PV voltage	U_{maxPV}	27	(V)
PV module scc current	I_{sccPV}	8.3	(A)
PV open circuit voltage	U_{opc}	32.3	(V)
Price	P_{PV}	483	($)

Having chosen the PV panel, the following calculation results are obtained:

- Modules in parallel N_{parPV} = 4,
- Modules in series N_{serPV} = 2,
- Total PV modules N_{totPV} = 8.

3.8. Controller CTRL Sizing for PV System

PV systems equipped with battery banks require charge controllers to regulate the charging process. The controller is typically oversized by 25% to handle the maximum current generated by the PV system under peak irradiance conditions [14]. For the system under consideration, a 'Speciality Concept ASC' charge controller with nominal values of 24V/12A has been selected [18,19], resulting in the necessary of 2 controllers in parallel.

4. COMPARATIVE ANALYSIS FOR POWERING ICCP SYSTEMS FROM TWO DIFFERENT SOURCES

4.1. Cost Calculation for the Standalone PV-Based System

The solar-powered system with lead-acid battery banks requires an increased number of units due to the extensive storage period required, as there is no Diesel backup generator [14].

Taking into account the sizing calculations from Chapter 3, the total initial investment costs presented in Table 11 have been obtained.

It was considered that the costs of cables, measurement, protection, and control equipment are around $5,000. The labour costs for installing the system were estimated at 20% of the cost of the equipment included in the PV system [14].

Table 11. Total initial investment cost of the system with lead-acid batteries

	Number of units	**Cost/unit ($)**	**Investment Cost ($)**
PV	8	483	3864
BA	8	317	2536
CTRL	2	54	108
BA Ch	1	1500	1500
Misc.	1	5000	5000
Install			2602
TOTAL			**15610**

In the case of the system with lithium-based battery banks, although the number of BA is smaller, they are significantly more expensive, resulting in higher initial investment costs, as shown in Table 12.

Table 12. Total initial investment cost of the system with LIFePO4 batteries

	Number of units	**Cost/unit ($)**	**Investment Cost ($)**
PV	8	483	3864
BA	5	926	2536
CTRL	2	54	108
BA Ch	1	1500	1500
Misc.	1	5000	5000
Install			3020
TOTAL			**18122**

It is also considered that the lifespan of the power generation system for cathodic protection is 25 years. During this period, lead-acid battery banks BA must be completely replaced every 5 years [14]. Of course, this timeframe may vary depending on the number of charge-discharge cycles to which the BA is subjected.

Thus, the total costs over the entire system's entire lifespan are obtained and summarized in Table 13.

Table 13. Total lifespan cost of the system with lead-acid batteries

	Number of units	Cost/unit ($)	Investment Cost ($)
PV	8	483	7728
BA	8	317	12680
CTRL	2	54	108
BA Ch	1	1500	1500
Misc.	1	5000	5000
Install			2602
TOTAL			**27016**

It was considered that the costs of cables, measurement, protection, and control equipment are around $5,000. The labor costs for installing the system were estimated at 20% of the cost of the equipment included in the PV system [14].

In the case of the system with lithium-based battery banks, although the number of BA is smaller, they are significantly more expensive, resulting in higher initial investment costs, as shown in Table 14.

Table 14. Total initial investment cost of the system with LIFePO4 batteries

	Number of units	Cost/unit ($)	Investment Cost ($)
PV	8	483	3864
BA	5	926	2536
CTRL	2	54	108
BA Ch	1	1500	1500
Misc.	1	5000	5000
Install			3020
TOTAL			**18122**

Lithium-based battery banks (BA) have fewer BAs and must be replaced entirely every 10 years due to their superior performance compared to lead-acid batteries [20]. Thus, the system's entire lifespan costs are obtained and summarized in Table 15.

Table 15. Total lifespan cost of the system with LiFePO$ batteries

	Number of units	Cost/unit ($)	Investment Cost ($)
PV	8	483	7728
BA	5	926	9260
CTRL	2	54	108
BA Ch	1	1500	1500
Misc.	1	5000	5000
Install			3020
TOTAL			**26616**

From the calculations summarized in the tables above, it can be observed that although the initial investment in the battery storage subsystem is $2,513 higher, the operating costs over the system's entire lifetime are $400 lower, Fig. 4.

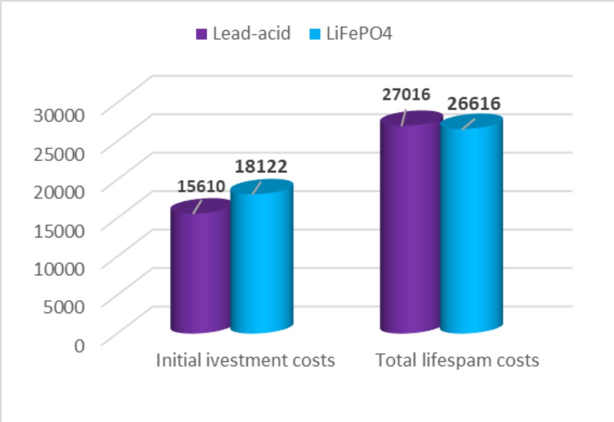

Fig. 4. PV system cost-effectiveness with two different battery types

4.2. Cost Calculation for the Grid Extension

Since, in this case study, the pipeline to be protected is considered to be located in a rural, open area without aesthetic or terrain restrictions, the LV network extension is carried out using an overhead power line (OHL) without the need for a new transformer station, the existing transformer already has a power reserve that covers the new energy requirements, Fig. 1.

The following costs for the components of the LV network extension were considered, see Table 16:

Table 16. Component costs for LV extension line [21]

Cost per unit	($)
Copper cable	3.13
Support pole	156.45
Connection strand	313.45
Measurement and protection unit	208.97
Electrical panel	417.94

Depending on the terrain and local conditions, the support poles for the OHL can be installed at intervals of 30 meters and 50 meters. In this study, we have considered these two cases as the lower cost is given by placing the poles every 50 meters, while the higher cost is given by placing the poles every 30 meters. The following costs for extending the LV electrical network to power the cathodic protection system have resulted, as shown in Table 17.

Table 17. LV extension costs with minimum, respectively, maximum number of electrical poles

Distance (km)	Min req. poles ($)	Max req. poles ($)
0.5	4070	5165
1	7200	9521
1.5	10328	13378
2	13457	18235
2.5	16586	22091
3	19715	26291
3.5	22843	30495
4	25973	34741
4.5	29102	38959
5	32231	43204

From Table 17, it can be observed that the costs of extension depend on the distance from the connection point, whereas the cost of the standalone system over its lifetime is fixed, Table 15.

4.3. Feasibility Analysis

For this case study, the PV system with lithium-based battery storage (LiFePO4) will be chosen because it ensures a more cost-effective and efficient energy storage solution over the system's lifetime. The cost of such a system over its 25-year lifespan has been calculated at $26,616, Table 15.

On the other hand, the costs of extending the LV (low voltage) electrical network depend on the distance from the connection point, while the lifecycle costs of the PV system with battery storage are fixed, Fig. 5.

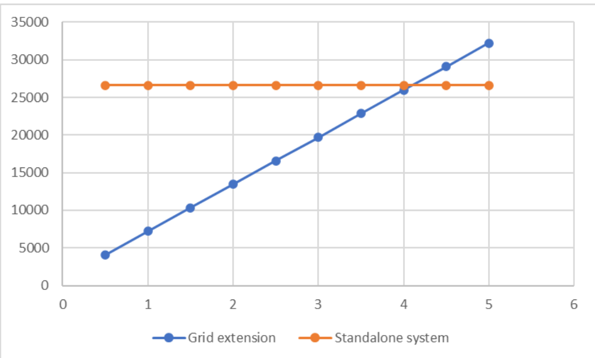

Fig. 5. CP electrification costs for minimum electric poles required

It can be observed from Fig. 5 that the standalone system becomes cost-effective when the power supply unit for CP current injection is located more than 4 km from the connection point of the grid to the LV electrical network.

In the case of extending the LV electrical line with a maximum number of poles required per kilometer, the power supply unit of the CP system must be located no more than 3 km from the connection point; above this distance, the PV system must be considered Fig. 6.

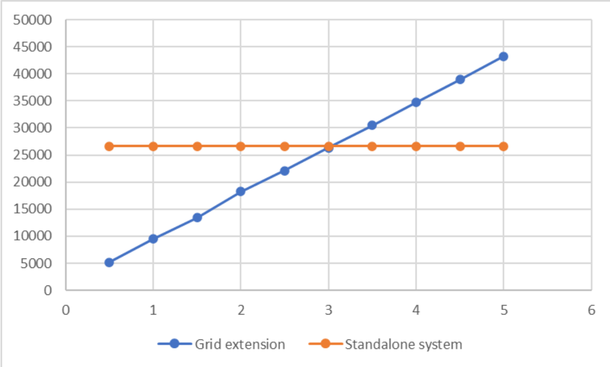

Fig. 6. CP electrification costs for maximum electric poles required

5. CONCLUSION

The power supply of ICCP systems for hydrocarbon transport pipelines located in isolated areas using renewable energy sources based on PV-BA tandem requires a careful design that must take into account the following:

- The most accurate determination of the total current required, the anode mass, and the daily load needed, the latter influencing the size of the electrical energy storage system in batteries.
- Obtaining the most accurate data regarding the availability of solar resources at the site, particularly solar irradiance and peak sun hours per day. The more precise these data are, the more the calculations of the design's current value and the optimal tilt angle of the PV panels will align with the actual conditions on the ground.
- The parameter of peak sun hours per day also influences the number of storage days, meaning the number of days the system will need to be powered by batteries due to unfavourable weather conditions. Generally, this number is higher than in hybrid PV systems because no backup Diesel generators are available.
- The choice of battery type for the storage subsystem is essential and directly influences the system's operating costs over its lifetime. These must be as maintenance-free as possible, stable in operation, performing better in low or high temperatures and with higher charging cycles.
- It is also preferable to have an accurate measurement of soil resistivity along all sections where the pipeline is installed in order to determine

how many additional current injection points for CP are needed beyond those obtained through calculations.

The feasibility of the two power supply solutions for the ICCP system stems from the fact that the costs of extending the electrical grid vary with the distance to the CP injection point. In contrast, the costs of powering the system with PV and batteries remain constant over the system's entire lifespan.

The study revealed that the break-even point depends on the cost of extending the power grid. The placement of support poles for the grid plays an important role and depends on the terrain configuration where the cathodic protection structure is located. If an additional transformer may be necessary, costs increase, further influencing the break-even point.

Powering ICCP systems using tandem PV systems and storage batteries is a viable solution for areas far from the national electricity grid, as these can replace, under site-specific conditions, the need to expand the existing electricity grid.

The success of powering ICCP systems from renewable resources largely depends on the most accurate collection of the availability of this resource on site. This design considers all factors influencing costs and precise measurements of soil resistivity along the pipeline.

Conflicts of Interest

The authors declare no conflict of interest.

REFERENCES

[1] S.S. Hosseini Dehshiri, B.Firoozabadi, Sustainable solar energy in urban areas: A novel framework for uncertainty, reliability, and 7E analysis. *Journal of Cleaner Production*, 444, 2024: 141136. https://doi.org/10.1016/j.jclepro.2024.141136

[2] Q. Yin, A. Li, C. Han, The Role of Solar Photovoltaic Roofs in Energy-Saving Buildings: Research Progress and Future Development Trends. *Buildings*, 14(10), 2024: 3091. https://doi.org/10.3390/buildings14103091

[3] K. Obaideen, M.N. AlMallahi, A.H. Alami, M. Ramadan, M.A. Abdelkareem, N. Shehata, A.G. Olabi, On the contribution of solar energy to sustainable developments goals: Case study on Mohammed bin Rashid Al Maktoum Solar Park. *International Journal of Thermofluids*, 12, 2021: 100123. https://doi.org/10.1016/j.ijft.2021.100123

[4] T.-Z. Ang, M. Salem, M. Kamarol, H.S. Das, M.A. Nazari, N. Prabaharan, A comprehensive study of renewable energy sources: Classifications, challenges and suggestions. *Energy Strategy Reviews*, 43, 2022: 100939. https://doi.org/10.1016/j.esr.2022.100939

[5] R. Ramanavasu, K. Vijayakumar, S.G. Fernandez, Integrated Nanogrid for the Impressed Current Cathodic Protection System in Desalination Plant. *Sustainability*, 15(9), 2023: 7088. https://doi.org/10.3390/su15097088

[6] R. Ekperi, M.U. Ajieh, S.C. Ikpeseni, H.I. Owamah, L.C. Edomwonyi-Otu, F. Okafor, Application of solar photovoltaic electricity in unravelling the effects of coating defects on cathodic protection parameters of buried pipeline. *IOP Conference Series: Earth and Environmental Science*, 1178, 2023: 012002. https://doi.org/10.1088/1755-1315/1178/1/012002

[7] K. Sun, W. Zhong, S. Huang, X. He, W. Cai, R. Ma, T. Jiang, S. You, L. Wang, W. Li, Research Progress on the Corrosion Mechanism and Protection Monitoring of Metal in Power Equipment. *Coatings*, 15(2), 2025: 119. https://doi.org/10.3390/coatings15020119

[8] G.-L. Song, The Grand Challenges in Electrochemical Corrosion Research. *Frontiers in Materials*, 1, 2014. https://doi.org/10.3389/fmats.2014.00002

[9] J.P. Guyer, An Introduction to Impressed Current Cathodic Protection. *Createspace Independent Publishing Platform*, 2014.

[10] V. Cicek, Corrosion Engineering and Cathodic Protection Handbook: With Extensive Question and Answer Section. *Wiley,* 2017.

[11] Photovoltaic Geographical Information System. *European Commission, Joint Research Centre Energy Efficiency and Renewables Unit.* https://re.jrc.ec.europa.eu/pvg_tools/en/ (Accessed: 13 January 2025).

[12] M.E. Parker, E.G. Peattie, Pipeline Corrosion and Cathodic Protection. *Elsevier BV*, 1988. https://doi.org/10.1016/C2011-0-06941-7

[13] Ș. Bunda, Specific aspects in the design of hybrid systems powering the telecommunications towers. *Journal of Sustainable Energy*, 15(1), 2024: 6-12.

[14] Stand-Alone Photovoltaic Systems: A Handbook of Recommended Design Practices, SAND87-7023, Rev. Nov 1991. *Sandia National*

Laboratories, Albuquerque, New Mexico, 1991.

[15] R.A. Kusmaya, T.R. Sahroni, Technical-economic feasibility of solar cathodic protection. *IOP Conference Series: Earth and Environmental Science*, 195, 2018: 012045. https://doi.org/10.1088/1755-1315/195/1/012045

[16] Trojan T105 Deep cycle lead-acid Battery, *Trojan Battery Company.* https://www.trojanbattery.com/products/t-105-6v-flooded-battery (Accessed: 13 January 2025).

[17] Controllers for PV hybrid systems, Technicalatasheet. http://specialtyconcepts.com/specialty_concepts_pdf_files/sc1_spec_sheet.pdf (Accessed: 13 January 2025).

[18] G. Blokdyk, Low-voltage network. *5STARCooks*, 2022.

[19] S.L. Herman, Electrical Wiring Industrial. *Cengage Learning*, 2017.

[20] Ș. Bunda, Influence factors in designing water pumping systems for remote rural consumer. *Journal of Sustainable Energy*, 13(1), 2023: 17-23.

[21] Component costs for LV network extension, *MWM Gas&Energy.* https://mwmgasenergy.ro/ce-trebuie-sa-verifici-inainte-de-a-extinde-o-retea-de-joasa tensiune-intr-un-cartier-nou/ (Accessed: 13 January 2025).